Bull. Mater. Sci., Vol. 39, No. 4, August 2016, pp. 1127–1132. © Indian Academy of Sciences.
DOI 10.1007/s12034-016-1232-9

# Slow evaporation method and enhancement in photoluminescence properties of $YPO_4 : Eu^{3+}$ co-doped with $Bi^{3+}$ ions

**K A KOPARKAR* and S K OMANWAR**
Department of Physics, Sant Gadge Baba Amravati University, Amravati 444 602, India

MS received 31 May 2015; accepted 1 February 2016

**Abstract.** **The series of $Bi^{3+}$ co-doped $YPO_4 : Eu^{3+}$ nanophosphors were successfully synthesized by the slow evaporation method. $Bi^{3+}$-doped and un-doped $YPO_4 : Eu^{3+}$ phosphors were characterized by using powder X-ray diffraction, Fourier transform infrared spectroscopy and field emission scanning electron microscopy. Photoluminescence (PL) properties and decay time of phosphors were studied at room temperature. The $YPO_4 : Eu^{3+}$ and $Bi^{3+}$ exhibit enhancement in PL intensity and quenched at 0.5 mol% of $Bi^{3+}$ ions.**

**Keywords.** **Slow evaporation method; $YPO_4 : Eu^{3+}, Bi^{3+}$; quenching effect; optical material.**

## 1. Introduction

The rare earth (RE) ions doped in yttrium-based inorganic nanophosphors are widely used as a host in various fields such as light-emitting devices, low-threshold lasers, optical amplifiers, biological fluorescence labels and drug-release schemes because nanophosphors much differ in physical and chemical properties than the bulk phosphors [1–4]. Thus, now-a-days, the practical world demands for highly efficient nanophosphors and hence enhancement in synthesis routes and their fluorescence properties are the main aspects of the studies. Also, the applied synthesis should be of low cost and produce highly beneficial improvement for various applications [5]. It is noticed that most of the researchers utilize co-dopants for increasing the efficiency of the phosphors like-wise, co-doping of $Bi^{3+}$ ions improves the luminescence intensity of $Eu^{3+}$-doped compounds such as $CaMoO_4 : Bi^{3+}$, $Eu^{3+}$ [6], $(Y,Gd)(P,V)O_4 : Eu^{3+}$, $Bi^{3+}$ [7], $GdNbO_4 : Eu^{3+}$, $Bi^{3+}$ [8]. This is because of the energy transfer from $Bi^{3+}$ to $Eu^{3+}$ ions ($Bi^{3+}$ acts as a sensitizer, whereas $Eu^{3+}$ acts as an activator) [9–11].

It is well known that yttrium-based phosphors are widely studied in the field of luminescence and mostly used in various display applications. So, most of the studies of enhancement and improvement are carried out with the yttrium-based materials. Most of the researchers studied the effect of $Bi^{3+}$ co-doping on the luminescence properties of yttrium-based phosphors such as $Y_2O_3 : Eu^{3+}, Bi^{3+}$, $YVO_4 : Eu^{3+}, Bi^{3+}$, $LnVO_4 : Eu^{3+}, Bi^{3+}$ on UV excitation for various synthesis methods [12–14]. For synthesis of such effective phosphors, most of the researchers used various non-conventional techniques such as sol–gel method [15], combustion synthesis [16], hydrothermal method [17], etc. and the advantages of these methods were controlling particle size, homogeneity, low cost, etc. But they have some drawbacks such as in sol–gel and hydrothermal methods, such as drying and annealing processes have to be slow and deliberate otherwise cracks and striations will appear in the samples and it is difficult to completely remove the residual hydroxyls from the phosphors [18]. Similarly in combustion synthesis, fuel and oxidizer is required and also it is very difficult to maintain the fuel/oxidizer ratio. In co-precipitation method, drying and washing processes are required, additionally, it requires precipitation agent [19]. To overcome the drawbacks of these methods is the key area of research and to produce a high quality phosphor is the main aspect of this work.

To the best of our knowledge, photoluminescence (PL) properties of $Bi^{3+}$ co-doped $YPO_4 : Eu^{3+}$ phosphors are synthesized by using more efficient synthesis method known as slow evaporation method. The synthesis through the slow evaporation method is low cost, low temperature and there is no need of any other agent for the initiation of synthesis process. Also, the processes like drying and annealing can be omitted. However, this method results in outstanding luminescent-intensity phosphor, which is main accomplishment of the present work.

## 2. Experimental

### 2.1 *Synthesis*

$Bi^{3+}$ co-doped $YPO_4 : Eu^{3+}$ phosphor was prepared by the slow evaporation method [20,21]. The stoichiometric amounts of high purity $Y_2O_3$ (AR) and $Eu_2O_3$ (AR) were dissolved in concentrated $HNO_3$ with deionized water. The resulting solution was considered as $Y(NO_3)_3 : Eu$. To this nitrate solution, appropriate molar concentration of $Bi(NO_3)_3$ was mixed. Then, stoichiometric amounts of $(NH_4)_2HPO_4$ (AR) was dissolved in deionized water and

*Author for correspondence (kakoparkar@gmail.com)

added dropwise. The entire homogeneous soluble solution was then placed on hot plate at 70°C for slow evaporation of water. To complete evaporation of water, dried precursor was finally crushed and heated at 900°C to get white crystalline powder of $YPO_4 : Eu^{3+}, Bi^{3+}$. The same process was carried out in the synthesis of all the samples.

### 2.2 *Characterization of samples*

The phase purities of $YPO_4 : Eu^{3+}$ samples were studied using Rigaku miniflex II X-ray diffractometer with scan speed of 2.000° per min and CuK$\alpha$ ($\lambda = 1.5406$ Å) radiation operating at 40 kV and 60 mA in the range of 10–90°. The morphology and chemical components of the as-prepared sample were characterized by using field emission scanning electron microscopy (FESEM, JEOL JSM-7500F) and Fourier transform infrared spectroscopy (FTIR, ALPHA FTIR spectrometer in the range of 4000–500 $cm^{-1}$). PL and PL excitation (PLE) spectra were measured on Hitachi F-7000 Spectrofluorometer in the range of 200–700 nm at room temperature. The parameters such as spectral resolution, width of the monochromatic slits (1 nm), photomultiplier tube (PMT) detector voltage and scan speed were kept constant throughout the analysis of samples.

## 3. Results and discussion

### 3.1 *Structural properties*

The formation of crystalline phase of the $YPO_4$ prepared by the slow evaporation method was confirmed by X-ray diffraction (XRD) pattern as shown in figure 1. The XRD pattern for $YPO_4 : Eu^{3+}, Bi^{3+}$ agreed well with the standard data from ICDD file (01-084-0335). The more significant and refined XRD pattern is represented in figure 1, where the background was subtracted from originally observed XRD pattern. The less background and high crystalline nature support the formation of desired $Y_{0.99}PO_4 : {}_{0.01}Eu^{3+}$ phase. Also, the XRD shows that the formed material was completely crystalline and was in single phase, where $a = b = 6.8817$ and $c = 6.0177$ Å. The space group for $YPO_4$ was I41/amd(141). Moreover,

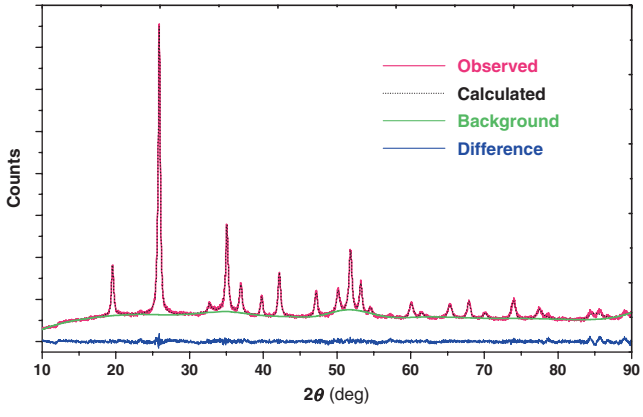


**Figure 1.** Refined XRD pattern for $YPO_4 : Eu^{3+}$ phosphor.

as shown in figure 2, there was no significant effect observed by increasing concentration of $Bi^{3+}$ in $YPO_4 : Eu^{3+}$.

The average crystallite size of $YPO_4 : Eu^{3+}$ and $YPO_4 : Eu^{3+}, Bi^{3+}$ phosphor determined from the Debye–Scherrer formula [22]. The crystalline size of $YPO_4 : Eu^{3+}$ and $YPO_4 : Eu^{3+}, Bi^{3+}$ was found to be 62.32 and 75.13, respectively.

### 3.2 *FTIR spectra of $YPO_4 : Eu^{3+}$ and $YPO_4 : Eu^{3+}, Bi^{3+}$ nanophosphors*

Figure 3 shows the FTIR transmittance spectra of $YPO_4 : Eu^{3+}$ and $Bi^{3+}$ (0.005 mole) co-doped $YPO_4 : Eu^{3+}$ nanophosphor in the frequency region of 500–4000 $cm^{-1}$. Both spectra show almost same nature except an extra peak in $YPO_4 : Eu^{3+}, Bi^{3+}$. The IR absorption peaks of $(PO_4)^{3-}$ are smaller than 643.13 $cm^{-1}$ corresponding to bending vibrations and peak at 1015.42 and near to the 1250 $cm^{-1}$ were strong bands corresponding to stretching vibrations. Also, transmittance spectra shows there was no C–O (around 1500 $cm^{-1}$) and O–H (around 3400 $cm^{-1}$) absorption band [23].

### 3.3 *FESEM images of $YPO_4 : Eu^{3+}$ and $YPO_4 : Eu^{3+}, Bi^{3+}$ nanophosphors*

Figure 4 shows FESEM images of $YPO_4 : Eu^{3+}$ and $Bi^{3+}$ (0.005 mol) co-doped $YPO_4 : Eu^{3+}$ nanophosphors. Both the phosphors consist of irregular grains with agglomerate phenomena. The agglomeration in grain was produced due to the time given for re-crystallization of solution by slow evaporation. It was also observed that the grains get finer and shaped in co-doped phosphor as compared to $Eu^{3+}$-doped phosphor. The average size of the particles was observed to be about 50–100 nm. The particle size obtained from FESEM was in concurrence with XRD analysis.

### 3.4 *PL properties*

Figure 5 shows combine emission and excitation spectra of $YPO_4 : Eu^{3+}$ phosphor prepared by the slow evaporation

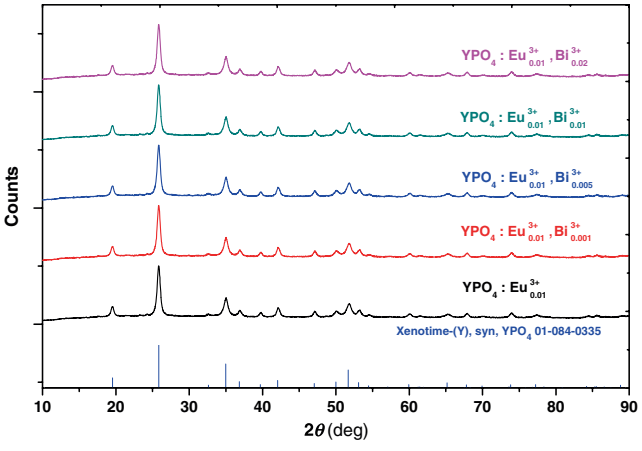


**Figure 2.** XRD patterns of $Y_{(0.99-y)}PO_4 : {}_{0.01}Eu^{3+}, {}_{y}Bi^{3+}$ ($y = 0.0, 0.001, 0.005, 0.01$ and 0.02).

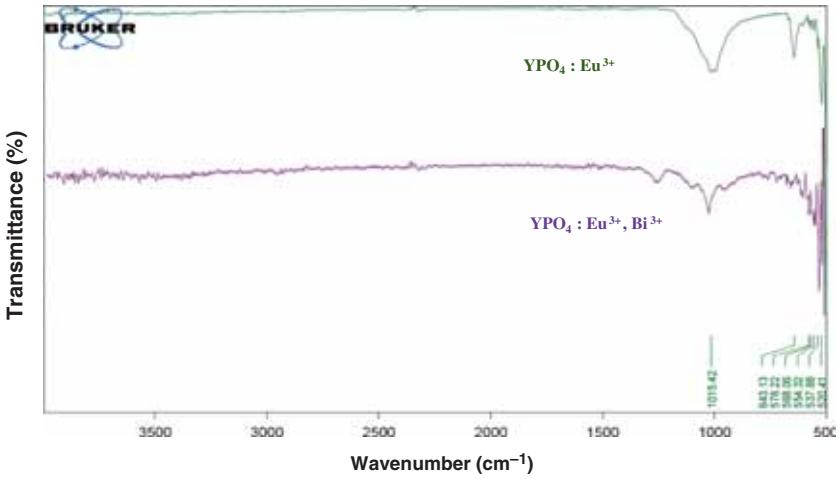


**Figure 3.** FT-IR spectra of $YPO_4 : Eu^{3+}$ and $YPO_4 : Eu^{3+}, Bi^{3+}$ nanophosphors.

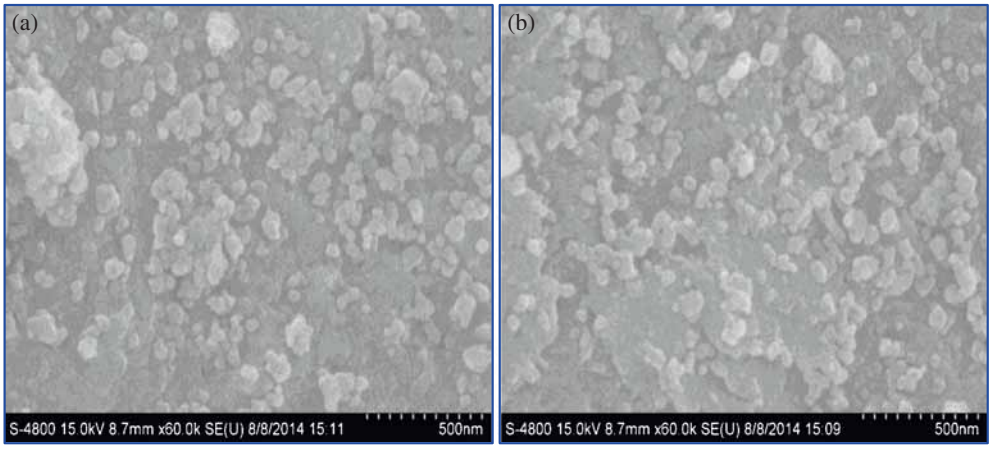


**Figure 4.** SEM images of (**a**) $YPO_4 : Eu^{3+}$ and (**b**) $YPO_4 : Eu^{3+}, Bi^{3+}$ nanophosphors.

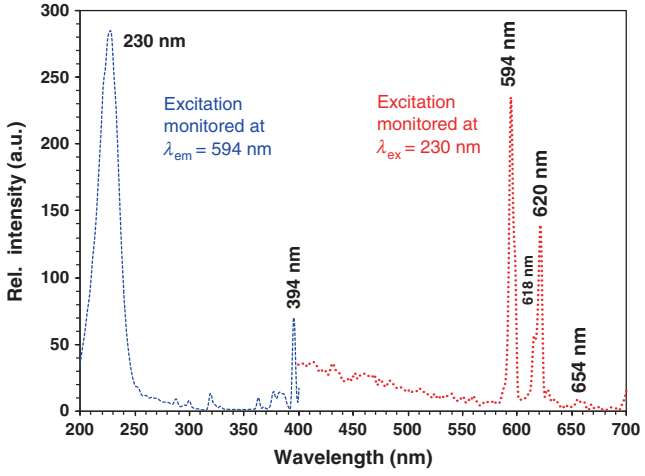


**Figure 5.** PL excitation and emission spectra of $YPO_4 : Eu^{3+}$ nanophosphors.

method. The excitation spectra consist of a broad band widening from 200 to 250 nm region of UV radiation and some sharp lines at near UV–Visible region. The broad band in UV region was attributed to fraction of the charge transfer band (CTB) of $O^{2-} \rightarrow Eu^{3+}$ bond [24]. The sharp lines which were observed within the $4f^6$ electron of $Eu^{3+}$ may be due to the f–f transitions, which were at near UV–Visible region. It was clearly seen that the emission spectra consist of two main peaks in the range of 550–700 nm corresponds to $^5D_0$ to $^7F_J$ ($J = 1$, 2 and 3) transitions of $Eu^{3+}$ monitored at 230 nm. The emission peak at 594 nm in orange region of visible spectrum was corresponding to magnetic dipole of $^5D_0 \rightarrow {}^7F_1$ transition, whereas the peak at 613 and 620 nm corresponding to $^5D_0 \rightarrow {}^7F_2$ transition of $Eu^{3+}$ ions which were due to the electric dipole transitions. The small peak observed at 654 nm which is corresponding to $^5D_0 \rightarrow {}^7F_3$ transition of $Eu^{3+}$ ions. The magnetic dipole transition exhibits more intense peak than electric dipole transition only when the impurity ion was situated at the inversion centre of the crystal.

Figure 6 shows the emission spectra of phosphors $Y_{(1-x)}PO_4 : {}_xEu^{3+}$-doped with different molar concentrations of $Eu^{3+}$ ($x = 0.005$, 0.01, 0.02 and 0.05) prepared by the slow evaporation method. For the entire samples, the

analysis condition was kept identical and the emission was monitored at excitation wavelength of 230 nm. The emission spectra exhibit the similar profile with different relative intensities. The emission intensity increases with the increase in $Eu^{3+}$ concentration. This implies that the dopant has not altered its position in the lattices with increase in concentration. Also, the dipole moments of the $Eu^{3+}$ were not affected by the increasing concentration.

All the excitation (monitored at 594 nm) and emission (monitored at 228 nm) spectra of $Y_{(0.99-y)}PO_4 : {}_{0.01}Eu^{3+}$, ${}_yBi^{3+}$ ($y = 0.02$, 0.01, 0.005, 0.001 and 0.0) is shown in figure 7. It was clearly seen that when percentage of $Bi^{3+}$ ions was 0.001 mole, as per the formula $Y_{(0.99-y)}PO_4 : {}_{0.01}Eu^{3+}$, ${}_yBi^{3+}$, the excitation peak slightly shifted towards shorter wavelength region from 233 to 228 nm and for further increase in concentration, the spectra remains at its position. But, intensity of the excitation spectra was affected by the variation in the concentration. From figure 7, it can be clearly seen that the emission intensity increased with increasing $Bi^{3+}$ concentration and concentration quenching observed at 0.005 mole of $Bi^{3+}$ concentration. Thus, optimum PL emission observed at molar concentration of $Bi^{3+}$ co-doped in $YPO_4 : Eu^{3+}$ was determined to be 0.005 mole. This implies that with co-doping of small amount of $Bi^{3+}$ in $YPO_4 : Eu^{3+}$, the absorption in the UV range and contribution to higher red light emission can be enhanced. This may be happened because of the energy transfer from $Bi^{3+}$ to $Eu^{3+}$ ions [25]. Beyond, by increasing $Bi^{3+}$ concentration, the emission intensity starts decreasing due to the sensitization effect of $Bi^{3+}$ ions on $Eu^{3+}$ ions.

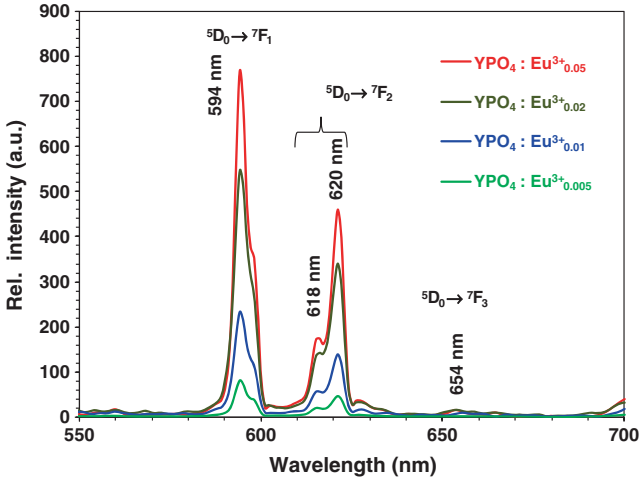


**Figure 6.** Emission spectra of $Y_{(1-x)}PO_4 : {}_xEu^{3+}$ nanophosphors ($x = 0.005$, 0.01, 0.02 and 0.05) under 230 nm excitation.

Higher concentration of $Bi^{3+}$ ions in the cluster may result into aggregation, which acts as trapping centres and scatter the absorbed energy nonradioactively, instead of transferring it to the $Eu^{3+}$ activator ions [26]. Therefore, more intense red emission could be observed by small amount of $Bi^{3+}$ as a co-dopant in $YPO_4 : Eu^{3+}$ phosphor.

The effect of $Bi^{3+}$ co-doped $YPO_4 : Eu^{3+}$ (Bi = 0.001, 0.005, 0.01 and 0.02) phosphors on the relative PL emission intensity of the magnetic dipole transition (594 nm) and electronic dipole transition (620 nm) are shown in figure 8. The results show that as the concentration of $Bi^{3+}$ increases, the luminescent intensity also increases and reaches the highest intensity when the doping concentration of $Bi^{3+}$ increases to 0.005 mol. However, the luminescent intensity decreases with increasing concentration of $Bi^{3+}$ in $YPO_4 : Eu^{3+}$ due to concentration quenching.

The relative PL intensity ratio for emission levels of $YPO_4 : Eu^{3+}$ and $YPO_4 : {}_{0.01}Eu^{3+}$, $Bi^{3+}$ phosphors corresponding to respective transitions are given in tables 1 and 2. From the values, it was clearly observed that as the percentage of $Eu^{3+}$ ions increases in $YPO_4 : Eu^{3+}$, the R/O ratio of $^5D_0 \rightarrow {}^7F_2$ to $^5D_0 \rightarrow {}^7F_1$ transition was linearly increased. Also, the R/O ratio increases by increasing doping concentration of $Bi^{3+}$ ions ($Eu^{3+}$ ions was fixed) [27,28].

The luminescence decay curves for $Bi^{3+}$ ions co-doped in $YPO_4 : Eu^{3+}$ phosphor are shown in figure 9. All the decay time curves were obtained by keeping the excitation wavelength at 228 nm and emission wavelength at 594 nm

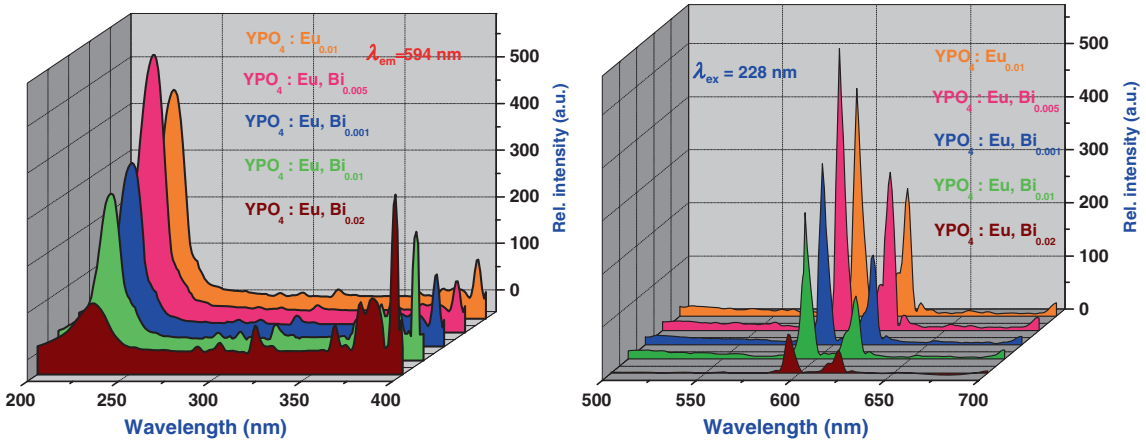


**Figure 7.** Excitation and emission spectra of $Y_{(0.99-y)}PO_4 : {}_{0.01}Eu^{3+}$, ${}_yBi^{3+}$ ($y = 0.0$, 0.001, 0.005, 0.01 and 0.02).

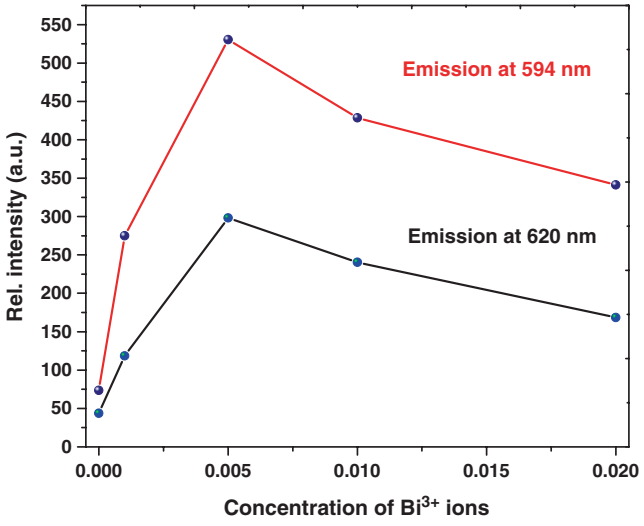


**Figure 8.** Peak intensity *vs.* concentration of $Bi^{3+}$ co-doped in $YPO_4 : Eu^{3+}$ nanophosphors ($\lambda_{ex} = 228$ nm).

**Table 1.** Relative PL intensity ratio of $YPO_4 : Eu^{3+}$ (by increasing doping concentration of $Eu^{3+}$).

| Phosphors | $^5D_0 \rightarrow {}^7F_2/{}^5D_0 \rightarrow {}^7F_1$ (R/O ratio) |
|---|---|
| $YPO_4 : {}_{0.005}Eu^{3+}$ | 0.772 |
| $YPO_4 : {}_{0.01}Eu^{3+}$ | 0.776 |
| $YPO_4 : {}_{0.02}Eu^{3+}$ | 0.816 |
| $YPO_4 : {}_{0.05}Eu^{3+}$ | 0.818 |

**Table 2.** Relative PL intensity ratio of $YPO_4 : Eu^{3+}$, $Bi^{3+}$ (by increasing doping concentration of $Bi^{3+}$ at constant doping concentration of $Eu^{3+}$).

| Phosphors | $^5D_0 \rightarrow {}^7F_2/{}^5D_0 \rightarrow {}^7F_1$ (R/O ratio) |
|---|---|
| $YPO_4 : {}_{0.01}Eu^{3+}$ | 0.776 |
| $YPO_4 : Eu_{0.01}, Bi_{0.001}$ | 1.686 |
| $YPO_4 : Eu_{0.01}, Bi_{0.005}$ | 1.784 |
| $YPO_4 : Eu_{0.01}, Bi_{0.01}$ | 2.026 |
| $YPO_4 : Eu_{0.01}, Bi_{0.02}$ | 2.320 |

($^5D_0 \rightarrow {}^7F_1$ transition). These curves can be well fitted using an equation, $I_t = I_0 \exp(-t/\tau)$, where $I_t$ and $I_0$ are the luminescence intensities at time $t = t$ and at time $t = 0$, and $\tau$ the decay time.

The maximum energy transfer from host or Eu–O CT band to $Eu^{3+}$ is responsible for their longer lifetime after excitation at ~228 nm because of high population of excited photons at the $^5D_0$ level. The obtained decay values in $YPO_4$ are in good agreement with reported values for $Eu^{3+}$ emission (2–3 ms) [29,30]. The doping concentration of $Bi^{3+}$ increases in $YPO_4 : Eu^{3+}$, then lifetime values are decreased and the calculated decay time $\tau = 3.295$, 3.299, 3.3631, 2.022 and 2.019 ms for $y = 0.0$, 0.001, 0.005, 0.01 and 0.02 mol of $Bi^{3+}$ in $YPO_4 : {}_{0.01}Eu^{3+}$, respectively.

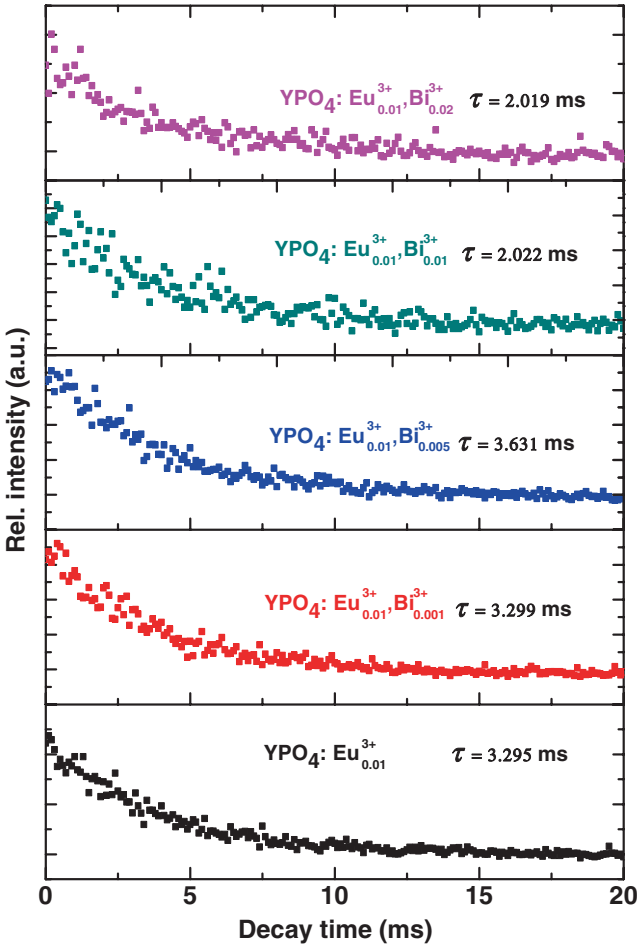


**Figure 9.** Emission decay time of $Bi^{3+}$ co-doped in $YPO_4 : Eu^{3+}$ nanophosphors.

## 4. Conclusions

$Bi^{3+}$ co-doped $YPO_4 : Eu^{3+}$ nanophosphors synthesized by the slow evaporation method which was low cost, low temperature and no other additive was required for the initiation of synthesis process. All the XRD patterns were similar in nature as the percentage of $Bi^{3+}$ ions increased in $YPO_4 : Eu^{3+}$. The $Bi^{3+}$ co-doped in $YPO_4 : Eu^{3+}$ gave brighter red PL emission spectra due to the energy transfer from $Bi^{3+}$ to $Eu^{3+}$ ions, but concentration quenching was observed at 0.005 mol of $Bi^{3+}$ ions in $YPO_4 : Eu^{3+}$. The decay time decreased with the increase in molar concentrations of $Bi^{3+}$ ions in $YPO_4 : Eu^{3+}$ phosphors, due to the energy transfer from $Bi^{3+}$ ions to $Eu^{3+}$ ions.

## Acknowledgement

Kishor A Koparkar would like to thank the Chairman of the FIST-DST Project at SGB Amravati University, Amravati, for providing XRD facility for this work.

## References


[1] Qina X, Jua Y, Bernhard S and Yao N 2007 *Mater. Res. Bull.* **42** 1440

[2] Luwang M N, Ningthoujam R S, Jagannath, Srivastava S K and Vatsa R K 2010 *J. Am. Chem. Soc.* **132** 2759

[3] Chen J, Meng Q, May P S, Berry M T and Lin C 2013 *J. Phys. Chem. C* **117** 5953

[4] Parchura A K and Ningthoujam R S 2012 *RSC Adv.* **2** 10854

[5] Chen L, Jiang Y, Yang Y, Huang J, Shi J and Chen S 2009 *J. Phys. D: Appl. Phys.* **42** 1

[6] Yan S, Zhang J, Zhang X, Lu S, Ren X, Nie Z *et al* 2007 *J. Phys. Chem. C* **111** 13256

[7] Pu Y, Tang K, Zhu D, Han T, Zhao C and Peng L 2013 *Nano-Micro Lett.* **5** 117

[8] Zhang D, Tang A, Yang L and Zhu Z 2012 *Int. J. Miner. Metall. Mater.* **19** 1036

[9] Wang M, Fan X and Xiong G 1995 *J. Phys. Chem. Solids* **56** 859

[10] Wei X T, Chen Y H, Cheng X R, Yin M and Xu W 2010 *Appl. Phys. B: Lasers Opt.* **99** 763

[11] Iso Y, Takeshita S and Isobe T 2014 *J. Phys. Chem. C* **118** 11006

[12] Chi L S, Liu R S and Lee B J 2005 *J. Electrochem. Soc.* **152** J93

[13] Xia Z, Chen D, Yang M and Ying T 2010 *J. Phys. Chem. Solids* **71** 175

[14] Park W J, Jung M K, Im S J and Yoon D H 2008 *Colloids Surf. A* **313** 373

[15] Huang J, Gao R, Lu Z, Qian D, Li W, Huang B and He X 2010 *Opt. Mater.* **32** 857

[16] Koparkar K A, Bajaj N S and Omanwar S K 2014 *Adv. Opt. Technol.* ID 706459. DOI:10.1155/2014/706459

[17] Lai H, Du Y, Zhao M, Sun K and Yang L 2014 *Ceram. Int.* **40** 1885

[18] Gowd G S, Patra M K, Songara S, Shukla A, Mathew M, Vadera S R *et al* 2012 *J. Lumin.* **132** 2023

[19] Lai H, Bao A, Yang Y, Xu W, Tao Y and Yang H 2008 *J. Lumin.* **128** 521

[20] Joseph V, Santhanam V, Gunasekaran S, Sagayaraj P and Ponnusamy S 2003 *Indian J. Pure Appl. Phys.* **41** 161

[21] Kawashima Y S, Gugliotti C F, Yee M, Tatumi S H and Mittani J R 2014 *Radiat. Phys. Chem.* **95** 91

[22] Koparkar K A, Bajaj N S and Omanwar S K 2015 *Indian J. Phys.* **89** 295

[23] Cao Y, Liu Y, Feng H and Yang Y 2014 *Ceram. Int.* **40** 15319

[24] Moura A P, Helena O L, Paris E C, Li M S, Andrés J, Varela J A *et al* 2011 *J. Fluoresc.* **21** 1431

[25] Wei X T, Chen Y H, Cheng X R, Yin M and Xu W 2010 *Appl. Phys. B* **99** 763

[26] Dong G, Hou C, Yang Z, Liu P, Wang C, Lu F *et al* 2014 *Ceram. Int.* **40** 14787

[27] Koparkar K A, Bajaj N S and Omanwar S K 2015 *Opt. Mater.* **39** 74

[28] Parchur A K, Ansari A A, Singh B P, Hasan T N, Syed N A, Rai S B *et al* 2014 *Integr. Biol.* **6** 53

[29] Parchur A K and Ningthoujam R S 2012 *RSC Adv.* **2** 10859

[30] Parchur A K, Ningthoujam R S, Rai S B, Okram G S, Singh R A, Tyagi M *et al* 2011 *Dalton Trans.* **40** 7595